Syntheses, Crystal Structures, and Electronic, ESR, and X-ray Photoelectron Spectra of Acetamidate- and 2-Fluoroacetamidate-Bridged Mixed-Valent Octanuclear Platinum Blues

Kazuko Matsumoto,*[1a] Ken Sakai,[1a] Kyosuke Nishio,[1a] Yasuhiro Tokisue,[1a] Reikichi Ito,[1a] Toshikazu Nishide,[1b] and Yushi Shichi[1c]

Contribution from the Department of Chemistry, Waseda University, Tokyo 169, Japan, Central Engineering Laboratories, Nissan Motor Co. Ltd., 1, Natsushima, Yokosuka, Kanagawa 237, Japan, and Nissan ARC Ltd., 1, Natsushima, Yokosuka, Kanagawa 237, Japan.
Received January 21, 1992

Abstract: The first mixed-valent octanuclear platinum blue compounds with bridging acetamidate and 2-fluoroacetamidate ligands, $[(H_3N)_2Pt(CH_3CONH)_2Pt(NH_3)_2]_4(NO_3)_{10}\cdot 4H_2O$ (**1**) and $[(H_3N)_2Pt(CH_2FCONH)_2Pt(NH_3)_2]_4(NO_3)_{8.66}\cdot 4H_2O$ (**2**), are crystallographically characterized. Compound **1** crystallizes in triclinic space group $P\bar{1}$, $Z = 1$, with $a = 12.091$ (2) Å, $b = 13.557$ (3) Å, $c = 10.983$ (4) Å, $\alpha = 100.62$ (2)°, $\beta = 97.12$ (2)°, $\gamma = 89.79$ (2)°, and $V = 1756$ (1) Å^3. Compound **2** crystallizes in triclinic space group $P\bar{1}$, $Z = 1$, $a = 12.214$ (5) Å, $b = 15.517$ (9) Å, $c = 10.794$ (4) Å, $\alpha = 106.86$ (4)°, $\beta = 97.92$ (3)°, $\gamma = 103.01$ (4)°, and $V = 1862$ (2) Å^3. Each octaplatinum complex cation is made up of a zigzag platinum chain formed by the tetramerization of four acetamidate-bridged head-to-head dimers. A new interdimer bonding mode, which has not been observed in the previous amidate-bridged tetranuclear compounds, is achieved between the N_4Pt and the N_2O_2Pt coordination planes in **1** and **2**. The Pt–Pt distances in **1**, 2.778 (1), 2.880 (2), 2.934 (1), and 2.900 (1) Å, are relatively shorter than those in **2**, 2.938 (6), 2.835 (5), 2.979 (5), and 2.962 (5) Å, probably due to the higher average platinum oxidation state of **1**. Compound **1** has been confirmed to be diamagnetic with ESR spectroscopy. The magnetic susceptibility measurement of **2** revealed that the compound has a magnetic moment of $\mu_{eff} = 1.41\ \mu_B$ and is a mixture of two isostructural compounds, diamagnetic $[(H_3N)_2Pt(CH_2FCONH)_2Pt(NH_3)_2]_4^{8+}$ and paramagnetic $[(H_3N)_2Pt(CH_2FCONH)_2Pt(NH_3)_2]_4^{9+}$, with the weight ratio of 65.77% for the latter. The diffuse reflectance spectrum of **1** shows strong broad absorption bands in the ranges of 450–650 nm with $\lambda_{max} = 500$ nm, 650–750 nm and at around 1200 nm with $\lambda_{max} = 1140$ nm. The former two bands in the visible region were also observed in the previously reported mixed-valent tetranuclear platinum blues, whereas the third absorption band in the near infrared region does not have its counterpart in the tetranuclear compounds. Extended Hückel molecular orbital calculation of **1** shows that all of the bands arise from the transitions between the MOs which have significant contributions of the Pt 5d-orbitals, and, therefore, the absorption bands can be regarded as the intervalence charge transfers between the Pt atoms. The X-ray photoelectron spectra of **1** and **2** exhibit Pt $4f_{5/2}$ and $4f_{7/2}$ binding energies at 76.5 and 73.3 eV for **1** and 76.4 and 73.4 for **2**, respectively. The comparison of the X-ray photoelectron spectra of several binuclear, tetranuclear, and octanuclear amidate-bridged platinum blue compounds with various average platinum oxidation states shows that, although the $4f_{7/2}$ binding energies of **1** and **2** are almost identical with those of the amidate-bridged Pt(II) binuclear compounds, the more broadened and less dented Pt $4f_{5/2}$ and $4f_{7/2}$ peak profiles compared to those of the binuclear and tetranuclear compounds suggest that several Pt(III) components overlap on the Pt(II) components in these octanuclear compounds.

Introduction

Since the original report of exceptionally dark blue platinum compound, first called "platinblau",[2] which was prepared from the reaction of $PtCl_2(CH_3CN)_2$ with $AgNO_3$, great progress has been made in the area of "platinum blues". Especially, since the discovery of the antitumor activity of *cis*-$PtCl_2(NH_3)_2$ (*cis*-DDP),[3] various platinum blues have been extensively studied for the reactions of the hydrolysis product of *cis*-DDP, i.e., *cis*-$[Pt(NH_3)_2(OH_2)_2]^{2+}$, with a variety of amidate ligands. Several *cis*-diammineplatinum pyrimidine blues were reported to possess high antitumor activities with lower nephrotoxicity than *cis*-DDP.[4] These studies have also provided a biochemical insight into the interactions between the hydrolysis products of *cis*-DDP and the purine and pyrimidine bases of DNA.

Although platinblau was found to have coordinated acetamide, derived from the hydrolysis of CH_3CN, and there had been several proposals[5,6] for the structure of the original platinblau, the structure of the compound still remained ambiguous. The first breakthrough in the platinum blue chemistry was the X-ray structure analysis[7] and the detailed characterization[6] of *cis*-diammineplatinum α-pyridone blue which revealed that the anomalously colored platinum compound is a mixed-valent tetranuclear platinum compound $[Pt_4(NH_3)_8(C_5H_6NO)_4]^{5+}$ (abbreviated as $Pt(2.25+)_4$) whose platinum oxidation state is formally expressed as $Pt^{II}_3Pt^{III}$, and the tetraplatinum chain structure is composed of two dimeric *cis*-$[Pt_2(NH_3)_4(C_5H_6NO)_2]^{n+}$ units having two amidate bridging ligands in a head-to-head arrangement (Scheme I, left). The one unpaired electron of the unusual oxidation state Pt(III) is delocalized over the four platinum atoms. Following these reports, several structural analogues with different platinum oxidation states, $Pt(2.0+)_4$ yellows,[8] $Pt(2.25+)_4$ blues,[9] and $Pt(2.5+)_4$ tan,[10]

(1) (a) Waseda University. (b) Central Research, Nissan Automobile Co. (c) Nissan ARC Ltd.
(2) Hofmann, K. A.; Bugge, G. *Ber.* **1908**, *41*, 312.
(3) (a) Rosenberg, B.; Van Camp, L.; Krigas, T. *Nature (London)* **1965**, *205*, 698. (b) Rosenberg, B.; Van Camp, L.; Trosko, J. E.; Mansour, V. H. *Nature (London)* **1969**, *222*, 385. (c) Rosenberg, B.; Van Camp, L. *Cancer Res.* **1970**, *30*, 1799.
(4) (a) Davidson, J. P.; Faber, P. J.; Fischer, R. G., Jr.; Mansy, S.; Peresie, H. J.; Rosenberg, B.; Van Camp, L. *Cancer Chemother. Rep.* **1975**, *59*, 287. (b) Rosenberg, B. *Cancer Chemother. Rep.* **1975**, *59*, 589.
(5) (a) Gillard, R. D.; Wilkinson, G. *J. Chem. Soc.* **1964**, 2835. (b) Brown, D. B.; Burbank, R. D.; Robin, M. B. *J. Am. Chem. Soc.* **1968**, *90*, 5621. (c) Brown, D. B.; Burbank, R. D.; Robin, M. B. *J. Am. Chem. Soc.* **1969**, *91*, 2895. (d) Laurent, M. P.; Tewksbury, J. C.; Krogh-Jespersen, M.-B.; Patterson, H. *Inorg. Chem.* **1980**, *19*, 1656.
(6) (a) Barton, J. K.; Best, S. A.; Lippard, S. J.; Walton, R. A. *J. Am. Chem. Soc.* **1978**, *100*, 3785. (b) Barton, J. K.; Caravana, C.; Lippard, S. J. *J. Am. Chem. Soc.* **1979**, *101*, 7269.
(7) (a) Barton, J. K.; Rabinowitz, H. N.; Szalda, D. J.; Lippard, S. J. *J. Am. Chem. Soc.* **1977**, *99*, 2827. (b) Barton, J. K.; Szalda, D. J.; Rabinowitz, H. N.; Waszczak, J. V.; Lippard, S. J. *J. Am. Chem. Soc.* **1979**, *101*, 1434.
(8) (a) Hollis, L. S.; Lippard, S. J. *J. Am. Chem. Soc.* **1981**, *103*, 1230. (b) Hollis, L. S.; Lippard, S. J. *J. Am. Chem. Soc.* **1983**, *105*, 3494. (c) Laurent, J.-P.; Lepage, P.; Dahan, F. *J. Am. Chem. Soc.* **1982**, *104*, 7335. (d) Hollis, L. S.; Lippard, S. J. *Inorg. Chem.* **1983**, *22*, 2600. (e) Matsumoto, K.; Miyamae, H.; Moriyama, H. *Inorg. Chem.* **1989**, *28*, 2959.

0002-7863/92/1514-8110$03.00/0

Scheme I

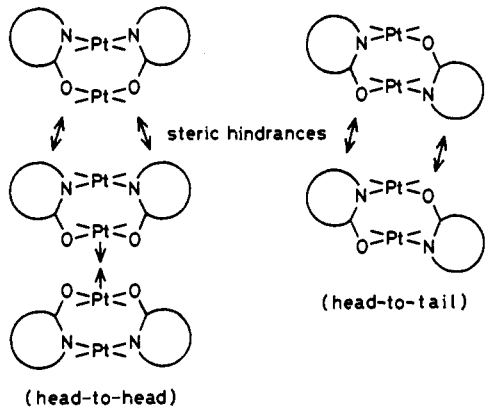

have been structurally characterized. A variety of platinum blue related binuclear complexes, head-to-head $Pt(2.0+)_2$[10b-d,11] and $Pt(3.0+)_2$[12] dimers, and head-to-tail (Scheme I, right) dimers[8a,12a,13] have also been reported.

All of these platinum blues and related complexes have been synthesized with lactam ligands, such as α-pyridone, 1-methylthymine, 1-methyluracil, or α-pyrrolidone, etc., and the tetraplatinum chain structures have been achieved only through the interdimer Pt–Pt bonding formations between the *cis*-(ammine-N)$_2$(amidate-O)$_2$ coordinated Pt atoms (N_2O_2Pt) of head-to-head (H–H) dimers. Interdimer bonding formation between the *cis*-(ammine-N)$_2$(amidate-N)$_2$Pt atoms (N_4Pt) of head-to-head dimers or between *cis*-(ammine-N)$_2$(amidate-N)(amidate-O)Pt atoms (N_3OPt) of head-to-tail (H–T) dimers have never been found. This fact has been explained by the steric bulk of the lactamate rings which hinders the formation of the Pt–Pt bondings between N_4Pt or N_3OPt atoms (Scheme I). However, the classical platinblau was synthesized with non-N-substituted chain amides, such as acetamide or trimethylacetamide, which have no such steric bulk at the N positions as those found in the cyclic amides. From a steric point of view, interdimer Pt–Pt bond formation between N_4–Pt or N_3OPt atoms can be expected in the platinum blues with non-N-substituted chain amidate ligands, and therefore we have studied the syntheses and the structures of platinum blues with acetamide and 2-fluoroacetamide as the bridging ligands.

As briefly reported in the preliminary communications,[14,15] we have recently solved the crystal structures of the platinum blues formed from the reactions of *cis*-$[Pt(NH_3)_2(OH_2)_2]^{2+}$ with acetamide and 2-fluoroacetamidate. We report here the preparations and the structural details of the first mixed-valent octanuclear platinum complexes with acetamidate (**1**) and 2-fluoroacetamidate (**2**) as the bridging ligands. The average platinum oxidation state of **1** and **2** have been determined to be 2.25+ and 2.0822+, respectively, with the measurements of the ESR spectra and the magnetic susceptibility. A new type of interdimer Pt–Pt bondings is achieved between the N_4Pt and the N_2O_2Pt atoms in both of the compounds, which demonstrates a large structural difference between cyclic lactamate and non-N-substituted chain amidate ligands. We also present the solid state UV–vis near infrared absorption and X-ray photoelectron spectra of the two compounds. The X-ray photoelectron spectra are also reported for α-pyrrolidonate and α-pyridonate bridged binuclear and tetranuclear compounds and the degree of the mixed valency is discussed with regards to the photoelectron spectra.

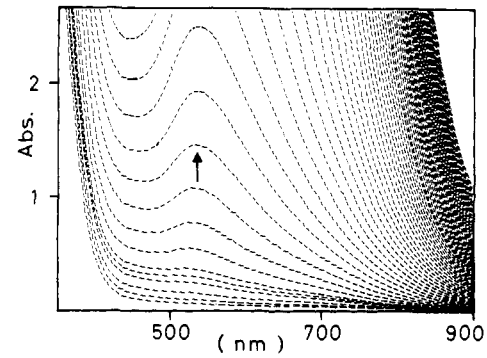

Figure 1. The spectral change during the platinum blue formation. An aqueous solution of 0.143 M *cis*-$[Pt(NH_3)_2(OH_2)_2](NO_3)_2$ and 0.148 M CH_3CONH_2 in a 1-cm quartz cell was reacted at 60 °C. Spectra were recorded every 10 min after 110 min of the reaction.

Experimental Section

Preparation of *cis*-Diammineplatinum Acetamide Blue, $[(H_3N)_2Pt(2.25+)(CH_3CONH)_2Pt(2.25+)(NH_3)_2]_4(NO_3)_{10}\cdot 4H_2O$ (1). Procedure A. An aqueous solution of *cis*-diamminediaquaplatinum dinitrate (1 mmol/7 mL), *cis*-$[Pt(NH_3)_2(OH_2)_2](NO_3)_2$,[16] was reacted with equimolar acetamide at 60–80 °C for 3–4 h in air. The synthesis was performed under normal room light. The solution gradually turned to blue-purple, as shown in Figure 1. The absorbance change at λ_{max} = 540 nm was slow at the initial stage but was faster as the reaction proceeded. The resulting blue-purple solution was gradually cooled to room temperature to form the red-purple crystals of the complex. After collecting the crystals by filtration, the filtrate was gradually concentrated at 5 °C to obtain the second crop. The crystalline sample was filtered off and dried in air. The yield was 28%. IR spectrum as KBr pellet: 3432 (br), 3268 (br), 2924 (w), 2856 (w), 2428 (w), 2324 (w), 1767 (w), 1604 (s), 1486 (s), 1384 (s), 1256 (s), 1040 (w), 960 (w), 864 (sh), 840 (w), 824 (w), 718 (br), 636 (w), 604 (w), 372 (w), cm^{-1}. Anal. Calcd for $Pt_8O_{42}N_{34}C_{16}H_{88}$: C, 6.43; H, 2.97; N, 15.93. Found: C, 6.60; H, 2.77; N, 15.49.

Procedure B. Suspension of *cis*-dichlorodiammineplatinum (1 mmol), silver nitrate (2 mmol), and acetamide (1 mmol) in 6 mL of water was heated with stirring in the dark (to avoid the light irradiation to the precipitating silver chloride) at 70 °C for 1 h and 45 min in Ar atmosphere. The solution was then cooled to room temperature to avoid further reaction and was filtered for removal of the AgCl. The filtrate was left at 5 °C to obtain the crystalline compound. The compound was 20%.

Procedure C. An addition of sodium nitrate (1.0 g) to the blue-purple solution prepared by the procedure A lead to immediate precipitation of the blue powder of the complex. The product was identified with IR spectroscopy and the elemental analysis. The yield was 23%.

Preparation of *cis*-Diammineplatinum 2-Fluoroacetamide Blue, $[(H_3N)_2Pt(2.0822+)(CH_2FCONH)_2Pt(2.0822+)(NH_3)_2]_4(NO_3)_{8.66}\cdot 4H_2O$ (2). An aqueous solution of 1 mmol of *cis*-$[Pt(NH_3)_2(OH_2)_2](NO_3)_2$ in 7 mL of H_2O was prepared according to the previous method.[16] To the solution was added 0.077 g (1 mmol) of 2-fluoroacetamide, and the solution was reacted at 40 °C for 2.5 days. After the solution was stored at 5 °C for 2 days, bluish-purple plate crystals appeared. Anal. Calcd for $Pt_8O_{37.98}F_8N_{32.66}C_{16}H_{80}$: C, 6.30; H, 2.64; N, 15.00. Found: C, 6.49; H, 2.39; N, 14.60. Since the crystals were rather unstable against X-ray irradiation, several attempts were made to obtain more stable crystals by exchanging the anion from NO_3^- to ClO_4^-, SiF_6^{2-}, BF_4^-, and PF_6^-. However, all the efforts resulted in vain and compound **2** was subjected to single-crystal X-ray diffraction study.

Preparations of the α-Pyrrolidonate- and α-Pyridonate-Bridged Binuclear and Tetranuclear Compounds. Binuclear and tetranuclear platinum blue related compounds with pyrrolidonate and α-pyridonate bridging ligands and with various average platinum oxidation states were prepared according to the previously reported methods for comparison of the X-ray

(9) O'Halloran, T. V.; Mascharak, P. K.; Williams, I. D.; Roberts, M. M.; Lippard, S. J. *Inorg. Chem.* **1987**, *26*, 1261.
(10) (a) Matsumoto, K.; Fuwa, K. *J. Am. Chem. Soc.* **1982**, *104*, 897. (b) Matsumoto, K.; Takahashi, H.; Fuwa, K. *Inorg. Chem.* **1983**, *22*, 4086.
(11) Lippert, B.; Neugebauer, D.; Schubert, U. *Inorg. Chim. Acta* **1980**, *46*, L11.
(12) (a) Hollis, L. S.; Lippard, S. J. *J. Am. Chem. Soc.* **1981**, *103*, 6761. (b) Hollis, L. S.; Lippard, S. *J. Inorg. Chem.* **1983**, *22*, 2605. (c) Lippert, B.; Schöllhorn, H.; Thewalt, U. *J. Am. Chem. Soc.* **1986**, *108*, 525. (d) O'Halloran, T. V.; Roberts, M. M.; Lippard, S. J. *Inorg. Chem.* **1986**, *25*, 957.
(13) (a) Lock, C. J. L.; Peresie, H. J.; Rosenberg, B.; Turner, G. *J. Am. Chem. Soc.* **1978**, *100*, 3371. (b) Faggiani, R.; Lock, C. J. L.; Pollock, R. J.; Rosenberg, B.; Turner, G. *Inorg. Chem.* **1981**, *20*, 804. (c) Schöllhorn, H.; Eisenmann, P.; Thewalt, U.; Lippert, B. *Inorg. Chem.* **1986**, *25*, 3384.
(14) Sakai, K.; Matsumoto, K. *J. Am. Chem. Soc.* **1989**, *111*, 3074.
(15) Sakai, K.; Matsumoto, K.; Nishio, K. *Chem. Lett.* **1991**, 1081.
(16) Lim, M. C.; Martin, R. B. *J. Inorg. Nucl. Chem.* **1976**, *38*, 1911.

photoelectron spectra with those of the octanuclear compounds (**1**) and (**2**). The compounds prepared were H-H $[(NO_3)Pt(3.0+)_2(NH_3)_4(C_4H_6NO)_2(NO_2)](NO_3)_2 \cdot H_2O$,[17] $[Pt(2.14+)_4(NH_3)_8(C_4H_6NO)_4](PF_6)_2(NO_3)_{2.56} \cdot 5H_2O$,[18] $[Pt(2.25+)_4(NH_3)_8(C_4H_6NO)_4](ClO_4)_2(NO_3)_3 \cdot 5H_2O$,[19] $[Pt(2.5+)_4(NH_3)_8(C_4H_6NO)_4](NO_3)_6 \cdot 2H_2O$,[10] and H-H $[Pt(2.0+)_2(en)_2(C_5H_4NO)_2](NO_3)_2$.[8d] All of the samples were microcrystalline state, and there is no doubt that the samples do not contain any traceable amount of contaminants.

Collection and Reduction of X-ray Data. A red-purple plate crystal of **1** (0.18 mm × 0.18 mm × 0.05 mm) and a bluish-purple plate crystal of **2** (0.13 mm × 0.13 mm × 0.03 mm) used in the X-ray diffraction study were coated with manicure, since the crystals were not stable against X-ray irradiation in air. The quality of each crystal was checked by measuring the peak profiles of several reflections on a four-circle single-crystal diffractometer ($\Delta w_{1/2} \leq 0.35°$ for **1** and $\Delta w_{1/2} \leq 0.40°$ for **2** for the reflections with $2\theta \leq 29°$). Unit cell parameters were refined with a least-squares fit of 24 reflections in the range of $20° < 2\theta < 25°$ for **1** and 25 reflections in the range of $25° < 2\theta < 30°$ for **2**. Intensity data were collected on a Rigaku AFC-5R diffractometer using graphite-monochromated Mo Kα radiation ($\lambda = 0.71068$ Å) at 25 °C. In spite of the employed crystal coatings, the average intensity of the three standard reflections still decreased by 4.2% for **1** and 8.3% for **2** at the end of the data collection. Therefore, analytical deterioration corrections were applied to the data with the intensities of the standard reflections collected every 200 reflections for **1** and every 100 reflections for **2**. Analytical absorption corrections were applied to the data by the method of North.[20] Further details of the data collection procedures are summarized in Tables I and S1.

Structure Solution and Refinement. The structures were solved by the direct method,[21] which revealed the positions of the four independent platinum atoms in the asymmetric unit for both **1** and **2**. All the remaining non-hydrogen atoms were located in the subsequent difference Fourier syntheses. All the non-hydrogen atoms were refined with anisotropic thermal parameters for **1**. The assignment of the coordinating oxygen and nitrogen atoms of the acetamidate ligand was not straightforward, since the C–N and C–O distances in the bridging ligand are almost equal, and, therefore, the two bonds are not easily discernible only by the bond lengths or the coordination mode of the ligands. The assignment was achieved by comparing the results of the final difference maps calculated for the two possible orientations of each acetamidate ligand. One of the orientations, which clearly gave lower R value and revealed the hydrogen atom, which is bonded to the acetamidate nitrogen atom, at a reasonable position, was selected as the right orientation of the ligand. This assignment of the ligand orientation and the detection of the ligand hydrogen atoms were possible for **1** but not for compound **2**, since the crystal deterioration during the data collection was more serious for **2**, compared to that of **1**. Therefore, the ligand orientation in **2** was determined in analogy to that of compound **1**. This assignment is supported by the close resemblance of the structures of **1** and **2** and the hydrogen bondings also observed in **2** between the bridged dimers. Only structurally important hydrogen atoms bonded to the acetamidate N atoms were located in the final difference synthesis and were refined with isotropic thermal parameters. All the calculations were carried out with the UNICS III program.[22] The atomic scattering factors were taken from ref 23, and the molecular and crystal structures were drawn with the ORTEP program.[24] Block-diagonal least-squares refinement of the structure for **1** with 468 parameters converged to $R = 0.0548$ and $R_w = 0.0860$, where $R = \sum||F_o| - |F_c||/\sum|F_o|$ and $R_w = [\sum w(|F_o| - |F_c|)^2/\sum w|F_o|^2]^{1/2}$, ($w = 1/\sigma^2(F_o)$). The largest peak in the final difference Fourier synthesis for **1** was 1.83 e/Å^3, except several larger peaks within 1.06 Å of the platinum atoms. The structure of **2** was refined with anisotropic temperature factors for Pt and F atoms and with isotropic ones for all the remaining non-hydrogen atoms, by a full-matrix least-squares method. The final refinement with 226 parameters converged to $R = 0.096$ and $R_w = 0.106$. The final largest peak in the difference Fourier synthesis was 2.30 e/Å^3, except several larger peaks within 1.60 Å of the Pt atoms. The final atomic positional and thermal parameters for **1** and **2** are deposited as supplementary material in Tables S2 and S3, respectively, and the interatomic distances and angles are shown in Tables S4 and S5. The anisotropic thermal parameters for **1** and **2** are listed in Tables S6 and S7, respectively, and the observed and calculated structure factors for **1** and **2** are in Tables S8 and S9, respectively. The torsion angles for **1** and **2** about the Pt–Pt axes are summarized in Tables S10 and S11 (supplementary material).

Physical Measurements. ESR spectra were recorded on a JEOL JES-RE2X X-band spectrometer operating at 3000 ± 1500 G with the microcrystalline samples. Since compounds **1** and **2** become more bluish on grinding, ESR and all other physical measurements were performed with microcrystalline samples without grinding. Single-crystal visible transmission and reflectance spectra were recorded on a Hitachi U-6000 microscopic spectrophotometer with a single crystal whose dimensions were less than 0.08 mm × 0.08 mm × 0.08 mm^3. The beam diameter was approximately 3 μm. The diffuse reflectance spectrum was measured on a Shimadzu UV3101PC spectrophotometer with a microcrystalline sample.

The X-ray photoelectron spectra were recorded on a VG Scientific Model ESCALAB MKII spectrometer. Mg Kα radiation (1253.6 eV) operated at 10 kV, and 20 mA was used as the X-ray excitation source. The microcrystalline samples were dispersed on a In film. The carbon 1s binding energy (284.6 eV) of the trace amount of hydrocarbon originally present in the air was used to calibrate the binding energy. The reproducibility of the measurement was 0.1 eV. Under these conditions the Ag $3d_{5/2}$ peak had a full width at half maximum (FWHM) value of 1.05 eV.

Magnetic susceptibility measurement was performed on a vibrating-sample magnetometer, Princeton Applied Research Model 4500, from 4.2 K to room temperature. The microcrystalline sample was placed in an alumina container and was used for the measurement.

Extended Hückel Molecular Orbital Calculation. EHMO calculation was carried out for **1c** with crystallographic C_i symmetry, based on the method in ref 25. All the coordinates of the atoms were taken from the result of the single-crystal X-ray structure analysis. The basic functions for the Pt atoms were referenced to the reported values.[26,27]

Results and Discussion

Synthesis. In the several synthetic procedures previously reported for the tetranuclear $Pt(2.25+)_4$ or $Pt(2.5+)_4$ complexes,[6-11] the initial pH values are adjusted in the range of 4.0–7.0 with NaOH to promote the deprotonation of the amides. However, no pH adjustment is necessary in the present synthesis of **1**, and the initial pH value was ca. 2.0. This low pH value is due to the hydrolysis of the coordinated water in the starting compound, *cis*-diaquadiammineplatinum complex. The blue solution can be similarly formed even in the presence of 1 M $HClO_4$. Acetamide seems to possess significantly higher coordination ability toward platinum atoms than the previously reported cyclic amides, such as α-pyridone, α-pyrrolidone, or 1-methyluracil in the substitution reaction of the coordinated water molecules in *cis*-$[Pt(NH_3)_2(OH_2)_2]^{2+}$. It is reported that coordination of acetamide–oxygen first occurs prior to the blue formation as suggested by ^{195}Pt NMR spectroscopy.[28]

An addition of nitric acid was always involved to promote the oxidation of the tetranuclear $Pt(2.0+)_4$ complexes formed at the initial stage, in the previous tetranuclear platinum blue syntheses.[6-11] However, no nitric acid is added additionally in the present case, and only nitrate anion exists as the counter anion of *cis*-$[Pt(NH_3)_2(OH_2)_2]^{2+}$ in the solution. Since the rate of oxidation, as observed with the rate of the coloration, is slightly slower but still fast enough when the solution is deaerated with Ar gas, the initially contained nitrate anion seems to act as the oxidizing agent.

In order to obtain the crystals of the complex at high yield, prolonged reaction at higher temperatures must be avoided. When the synthetic solution was heated at 80 °C for more than 5 h, no

(17) (a) Abe, T.; Moriyama, H.; Matsumoto, K. *Chem. Lett.* **1989**, 1857. (b) Abe, T.; Moriyama, H.; Matsumoto, K. *Inorg. Chem.* **1991**, *30*, 4198.
(18) Matsumoto, K.; Fuwa, K. *Chem. Lett.* **1984**, 569.
(19) Matsumoto, K. *Chem. Lett.* **1984**, 2061.
(20) North, A. T. C.; Phillips, D. C.; Mathews, F. S. *Acta Crystallogr.* **1968**, *A24*, 351.
(21) Main, P.; Woolfson, M. M.; Germain, G. *A Computer Programme for the Automatic Solution of Crystal Structures*; (revised) University of York, York, England and University de Louvain, Leuven, Belgium, 1971.
(22) Sakurai, T.; Kobayashi, K. *Rikagaku Kenkyusho Hokoku* **1979**, *55*, 69.
(23) *International Tables for X-ray Crystallography*; Kynoch Press: Birmingham, England, 1974; Vol. IV, p 99.
(24) Johnson, C. K.; *Report ORNL-3794* (revised), Oak Ridge National Laboratory: Oak Ridge, TN, 1965.
(25) Hoffman, R. *J. Chem. Phys.* **1964**, *40*, 2745.
(26) Tatsumi, K.; Hoffman, R.; Yamamoto, A.; Stille, J. K. *Bull. Chem. Soc. Jpn.* **1981**, *54*, 1857.
(27) Berke, H.; Hoffman, R. *J. Am. Chem. Soc.* **1978**, *100*, 7224.
(28) Kerrison, S. J. S.; Sadler, P. J. *J. Chem. Soc., Chem. Commun.* **1981**, 61.

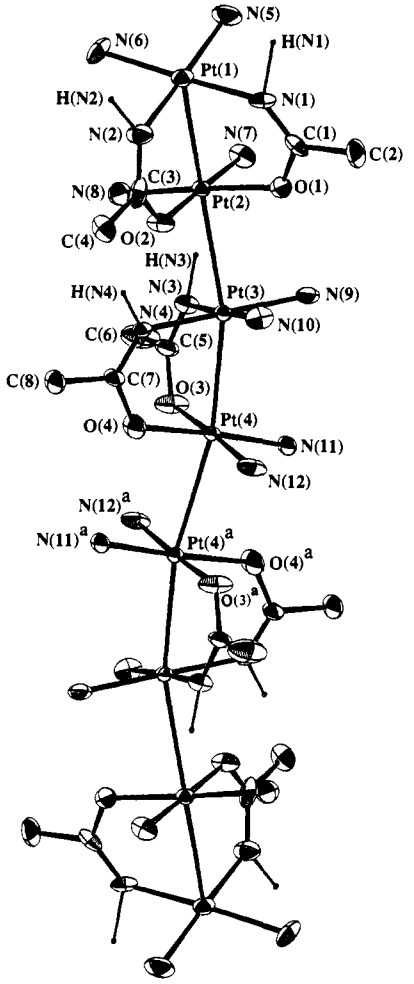

Figure 2. An ORTEP drawing and the atom labeling scheme for the octanuclear platinum cation, $[(H_3N)_2Pt(CH_3CONH)_2Pt(NH_3)_2]_4^{10+}$ (**1c**).

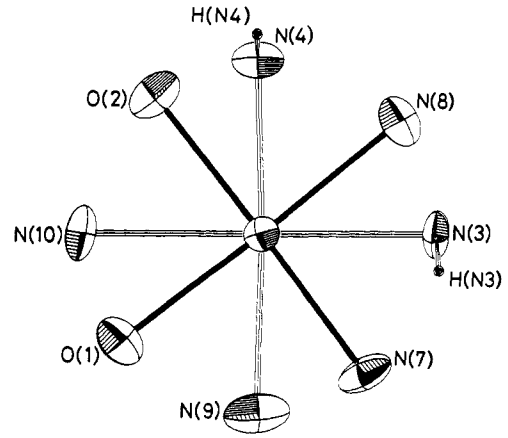

Figure 3. A newly-achieved interdimer bonding between $N_4Pt(2)$ and $N_2O_2Pt(3)$ in **1c**, as observed along the Pt(2)–Pt(3) vector.

Table I. Crystallographic Data

	1	2
chem formula	$Pt_8O_{42}N_{34}C_{16}H_{88}$	$Pt_8O_{37.98}F_8N_{32.66}C_{16}H_{80}$
fw	2989.92	3050.77
cryst syst	triclinic	triclinic
space group	$P\bar{1}$	$P\bar{1}$
cryst param		
a =	12.091 (2) Å	12.214 (5) Å
b =	13.557 (3) Å	15.517 (9) Å
c =	10.983 (4) Å	10.794 (4) Å
α =	100.62 (2)°	106.86 (4)°
β =	97.12 (2)°	97.92 (3)°
γ =	89.79 (2)°	103.01 (4)°
V	1756 (1) Å^3	1862 (2) Å^3
Z	1	1
T	25 °C	25 °C
λ	0.71068 Å	0.71068 Å
ρ calcd	2.828 g cm^{-3}	2.721 g cm^{-3}
μ	161.5 cm^{-1}	152.5 cm^{-1}
transm factors	0.602–1.000	0.713–1.000
R	0.055	0.096
R_w ($w = 1/\sigma^2(F)$)	0.086	0.106

crystal was obtained either upon cooling nor upon gradual concentration.

Description of the Structure of 1. The ORTEP drawing for the structure of the acetamidate-bridged *cis*-diammineplatinum blue cation is shown in Figure 2 with the atomic numbering scheme. The complex cation **1c** has an octanuclear platinum chain structure with a crystallographic inversion center at the midpoint of the Pt(4)–Pt(4)^a vector (for the superscript a, see the footnote of Table IV). The octameric structure is accomplished by three interdimer Pt–Pt bondings and hydrogen bondings between the four dimeric units. Each independent dimeric unit is doubly-bridged by acetamidate ligands in a head-to-head manner. The structure of the inner tetrameric Pt(3)–Pt(4)–Pt(4)^a–Pt(3)^a unit is similar to those of the reported tetranuclear $Pt(2.0+)_4$,[8] $Pt(2.25+)_4$,[7,9] or $Pt(2.5+)_4$[10] complexes.

The central interdimer Pt–Pt bonding of Pt(4)–Pt(4)^a (2.934 (1) Å) is reinforced by the four hydrogen bondings between the oxygen atoms of the acetamidate ligands and the nitrogen atoms of the ammine ligands, O(3)–N(12)^a = 2.85 (3) Å and O(4)–N(11)^a = 2.80 (3) Å, and this hydrogen bonding geometry resembles those of the previous tetranuclear platinum compounds. The central Pt–Pt distance is a little longer than the values of 2.866 (2)–2.9158 (5) Å for the cyclic-amidate coordinated $Pt(2.25+)_4$ blues, summarized in Table S5, but the central metal–metal bonding might be stronger than is considered from the apparent Pt–Pt distance, since the angle of Pt(3)–Pt(4)–Pt(4)^a = 168.78 (5)° is relatively linear and is close to the value of α-pyrrolidonate-bridged $Pt(2.5+)_4$ tan (Table S5).

The outer interdimer bonding between the $N_4Pt(2)$ and the $N_2O_2Pt(3)$ planes (Figure 3) demonstrates that an interdimer bonding for the *cis*-(ammine-N)$_2$(amidate-N)$_2$Pt plane is sterically possible and is realized in **1c**, which has been prohibited for the previous cyclic amidate-bridged compounds from the steric reason. The bonding of Pt(2)–Pt(3) (2.900 (1) Å) is also stabilized by the "W-shaped" four hydrogen bondings, two of which are strong, O(1)–N(10) = 2.98 (3) and O(2)–N(4) = 2.83 (3) Å, and the other two are relatively weak, O(1)–N(9) = 3.28 (4) and O(2)–N(10) = 3.07 (3) Å (Figures 2 and 3). One of the nitrogen atoms of the acetamidate ligands in the Pt(3) coordination plane, N(4), is involved in the hydrogen bonding, while the other N(3) is not. Therefore, the interaction between the Pt(2) and Pt(3) coordination planes (Figure 3) is somewhat different from those in the tetranuclear compounds, which is better expressed with the average torsional angle of 127.9° for O(1)–Pt(2)–Pt(3)–N(4), O(2)–Pt(2)–Pt(3)–N(3), N(7)–Pt(2)–Pt(3)–N(10), and N(8)–Pt(2)–Pt(3)–N(9) about the Pt(2)–Pt(3) vector and with the platinum torsion angle of Pt(1)–Pt(2)–Pt(3)–Pt(4) = 94.2 (2)°. In another view, supposing the two strong hydrogen bonds as the bridging ligands, the average torsional twist, ω, about the Pt(2)–Pt(3) vector is calculated to be 37.9°. The two coordination planes of the Pt(2) and Pt(3) are rotated to each other in a staggered form to avoid close contacts between the coordinating donor atoms (Figure 3). In spite of this rotation, the contacts of non-hydrogen-bonded nitrogen atoms, summarized in Table S4, are within relatively short distances, and the cant angle, τ, between the two coordination planes is a remarkably small value of 10.7°, suggesting a strong attractive interaction between the two planes.

The amidate-bridged Pt–Pt distances are different between the inner and the outer dimers. The inner Pt(3)–Pt(4) = 2.778 (1) Å is within the usual range of 2.7745 (4)–2.8296 (5) Å for the $Pt(2.25+)_4$ blues (Table II), suggesting that the actual platinum

Table II. Comparison of the Geometric Features of Amidate-Bridged Octanuclear and Tetranuclear Platinum Complexes

compound	formal Pt oxidn state	Pt–Pt dist, A	Pt–Pt–Pt angle, deg	τ,[a] deg	ω,[b] deg	ref
$[(H_3N)_2Pt(CH_3CONH)_2Pt(NH_3)_2]_4(NO_3)_{10}\cdot 4H_2O$ (1)	2.25	2.880 (2)[c]	163.77 (5)[d]	28.4	3.7	e
		2.778 (1)[c]	165.51 (4)[d]	10.7[d]	37.9[d]	
		2.900 (1)[d]	168.78 (5)	25.6	5.6	
		2.934 (1)				
		4.095 (2)[f]	161.21 (4)[g]			
$[(H_3N)_2Pt(CH_2FCONH)_2Pt(NH_3)_2]_4(NO_3)_{8.66}\cdot 4H_2O$ (2)	2.08	2.938 (6)[c]	161.8 (1)[d]	32.3	4	e
		2.835 (5)[c]	166.4 (2)[d]	8.3[d]	37[d]	
		2.962 (5)[d]	169.5 (1)		4	
		2.979 (5)				
		7.128 (7)[f]				
$[(H_3N)_2Pt(C_5H_4NO)_2Pt(NH_3)_2]_2(NO_3)_5\cdot H_2O$	2.25	2.7745 (4)[c]	164.20 (2)	27.4	22.8	6b
		2.8770 (9)				
		6.413 (3)[f]				
$[(H_3N)_2Pt(C_5H_5N_2O_2)_2Pt(NH_3)_2]_2(NO_3)_5\cdot 5H_2O$	2.25	2.810 (2)[c]	165.02 (5)	27.3	6.1	11
		2.866 (2)	164.81 (5)	26.4	8.4	
		2.793 (2)[c]				
		8.400 (3)[f]				
$[(en)Pt(C_5H_4NO)_2Pt(en)]_2(NO_3)_5\cdot H_2O$	2.25	2.8296 (5)[c]	164.33 (3)	32.1	24.3	12d
		2.9158 (5)				
		6.386 (2)[f]				
$[(H_3N)_2Pt(C_4H_6NO)_2Pt(NH_3)_2]_2(NO_3)_6\cdot 2H_2O$	2.5	2.702 (6)[c]	170.4 (1)	18.7	4.3	10b
		2.710 (5)	168.8 (1)	21.2	5.1	
		2.706 (6)[c]				
		7.538 (7)[f]				
$[(H_3N)_2Pt(C_5H_4NO)_2Pt(NH_3)_2]_2(NO_3)_4$	2.0	2.8767 (7)[c]	158.40 (3)	30.0	20.3	8a
		3.1294 (9)				
		6.9657 (8)[f]				
$[(H_3N)_2Pt(C_4H_6NO)_2Pt(NH_3)_2]_2(PF_6)_3(NO_3)\cdot H_2O$	2.0	3.029 (2)[c]	157.94 (5)	35.9	17.9	8e
		3.184 (2)				
		7.795 (3)[f]				
$[(en)Pt(C_5H_4NO)_2Pt(en)]_2(NO_3)_4$	2.0	2.9915 (4)[c]	160.58 (3)	39.6	24.9	8d
		3.2355 (5)				
		7.538 (1)[f]				

[a] Tilt angles between adjacent platinum coordination planes. [b] Average torsion angles about the Pt–Pt axes. [c] Amidate-bridged Pt–Pt distances. [d] Values for the Pt(2)–Pt(3) geometry in the present work, where ω is given with regards to the two strong hydrogen bonds. [e] This work. [f] The nearest intercationic Pt–Pt distances, calculated from the reported positional parameters. [g] A Pt(1)[b]–Pt(1)–Pt(2)–Pt(3) angle in the present work.

oxidation state of the inner two dimer units would be close to +2.25. On the other hand, the outer Pt(1)–Pt(2) = 2.880 (2) Å is a little longer and is rather comparable to the value of 2.8767 (7) Å in the α-pyridonate-bridged [*cis*-diammine$Pt(2.0+)]_4$ complex (Table II). However, the angle Pt(1)–Pt(2)–Pt(3) = 163.77° is still comparable to the values for the $Pt(2.25+)_4$ blues, and, therefore, the outer two dimeric units would also be partially oxidized. The several longer Pt–Pt bond distances in **1**, compared to those in $Pt(2.25+)_4$ blues, might be due to the extra Pt–Pt interaction, i.e., the intertetramer interaction, achieved at the Pt(4)–Pt(4)[a] bonding of the octamer. The platinum distances and the angles also suggest that Pt(3.0+) nature is higher in the inner Pt(3)–Pt(4) dimers of the octaplatinum chain.

All of the four independent platinum coordination planes are planar, where four-atom root-mean-square deviations are in the range of 0.019–0.028 Å. As in the case of the previous platinum blues and the related complexes, platinum atoms are displaced from their respective calculated best planes, regardless of the average oxidation state, in such a manner that each Pt atom in the bridged atom pairs Pt(1)/Pt(2) and Pt(3)/Pt(4) move closer toward each other. The largest shift of 0.084 Å from the best plane is found for the Pt(1) atom, indicating that Pt(1) is strongly attracted toward the Pt(2) atom. The shortest shift is found for the Pt(2) atom and is 0.018 Å, which is less than the deviations of 0.022–0.026 Å for the four coordinating atoms. The shift of 0.040 Å for the Pt(3) atom is relatively shorter as a value for the *cis*-$N(ammine)_2N(amidate)_2$-coordinated Pt atom, compared to the values of 0.075–0.099 Å for the reported $Pt(2.25+)_4$ blues (calculated from the reported positional parameters[7b,9] with the program system UNICS III). On the other hand, the Pt(4) atom has a relatively large shift of 0.054 Å, which leads to the long Pt(4)–Pt(4)[a] distance.

The tilt angles, τ, between the coordination planes within the dimer units are 28.4° and 25.6°, for the outer Pt(1)–Pt(2) and the inner Pt(3)–Pt(4) unit, respectively. The torsion angle in each dimeric unit is relatively small, and the average torsional twists are 3.7° and 5.6° about the Pt(1)–Pt(2) and the Pt(3)–Pt(4) vector, respectively.

The bite distances of the bridging acetamidate are normal, ranging from 2.27 (4) to 2.29 (3) Å, except for the short distance of N(4)–O(4) = 2.20 (3) Å. This short distance is due to the relatively short distance of N(4)–C(7) = 1.23 (4) Å, compared to other N–C distances which are in the range of 1.29 (4)–1.34 (4) Å. The exceptionally short N(4)–C(7) bond might be probably due to the fact that only the acetamidate ligand containing the N(4) atom is participating in the hydrogen-bonding interaction at both ends of the dimer unit and might be receiving a stronger strain compared to the rest of the acetamidate ligands. The angles in the acetamidate ligands are almost equivalent and are averaged into O–C–N = 122°, O–C–C = 116°, and N–C–C = 122°. The O–C–N bite angle is not significantly distorted upon bridging and is comparable to that of a free acetamide molecule (122°).[29] The average C–N distance of 1.30 Å shows a marked change upon deprotonation and complexation, compared to the free acetamide value of C–N = 1.38 Å[29] and is intermediate between the values of 1.255 Å for a pure C=N double bond[30] and 1.45 Å for a single C–N bond associated with an sp^2-hybridized carbon atom.[31]

In the crystal lattice, an octaplatinum cation is related to another one through a crystallographic inversion center with a Pt–Pt separation of 4.095 (2) Å (Figure 4). This intercationic Pt–Pt distance is much shorter than the values of the reported tetranuclear platinum complexes summarized in Table II. The relatively linear platinum angle of Pt(1)···Pt(1)–Pt(2) = 161.21° also suggests an expectation for the formation of a longer polynuclear platinum chain structure in the *cis*-diammineplatinum acetamide

(29) Denne, W. A.; Small, R. W. H. *Acta Crystallogr.* **1971**, *B27*, 1094.
(30) Nardelli, M.; Fava, G. *Acta Crystallogr.* **1962**, *15*, 214.
(31) Pauling, L. *The Nature of the Chemical Bond*, 3rd ed.; Cornell University Press: Ithaca, NY, 1960.

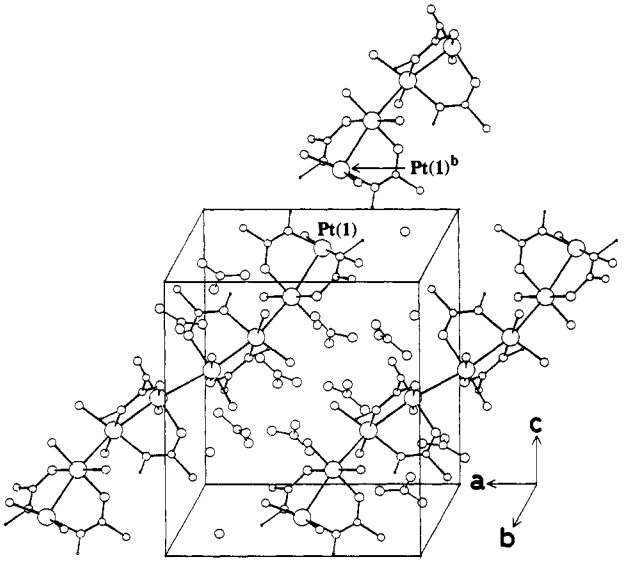

Figure 4. The crystal packing view and the intercationic relationship in **1**. The superscript b on Pt(1) is referred to as the footnote in Table IV. The atoms are expressed with balls of an equal diameter for clarity.

complex. However, the intercationic Pt···Pt distance is still too long to be considered as a metal–metal bonding. The inability of the $N_4Pt(1)$ and $N_4Pt(1)^b$ planes to form a hydrogen-bonding interaction between them indirectly suggests that a hydrogen bonding might be indispensable for the formation of a stable interdimer Pt–Pt bonding.

The nitrate anions and the water molecules are interposed between the cations, and the crystal packing is stabilized by an extensive hydrogen bonding network, as detailed in Table S4. Other structural details are also found in Table S4.

Description of the Structure of 2. The structure of **2c** is, as shown in Figure 5, basically similar to that of **1c**. However, the average Pt oxidation state of **2** is 2.0822, whereas that of **1** is 2.25, and, therefore, significant differences are observed in the Pt–Pt distances and angles. Only six nitrate anions per complex cation were found in the crystal lattice of **2**. The remaining nitrates seem to be disordered in the lattice and could not be located. The average Pt oxidation state of **2** was, therefore, determined with the magnetic susceptibility data as described later in this paper. As briefly discussed in the Experimental Section, due to the large deterioration of the crystal during the data collection, it was difficult to assign the right orientations of the bridging 2-fluoroacetamidate ligands. However, several intercationic hydrogen bonds observed have provided strong support for the determined arrangement of the four independent 2-fluoroacetamidate ligands. First, the observed directions of the F atoms, F(1), F(2), and F(4) having intraligand hydrogen bonding interactions with amidate nitrogen atoms, are in good agreement with the proposed amidate arrangements, except for one 2-fluoroacetamidate with F(3) atom which has a slightly longer interatomic distance of F(3)–O(3) = 2.6 (1) Å compared to those of the other three (see Figure 3 and Table S5). Secondly, the observed interdimer hydrogen bonds within an octaplatinum molecule are also in good agreement with the proposed arrangement. Therefore, three of the four 2-fluoroacetamidate ligands can be located, without any doubt, in the proposed manner which is analogous to **1**. Finally, we have concluded the orientation of the amidate ligand having F(3) atom to be analogous to **1**, since this orientation fits the interdimer hydrogen-bonding interactions observed in **2**. The exceptional direction of F(3) atom can be reasonably explained by the observed intercationic hydrogen bonding of F(3) with $N(8)^d$, F(3)–$N(8)^d$ = 3.0 (1) Å. The crystal packing of **2** (Figure 6) shows that the cations exist independently, and the linear arrangement of the cations as observed in **1** does not exist in **2**.

The bond distances and the angles in **2** are listed in Table S5. The corresponding Pt–Pt distances listed in Table II show that all the distances are longer by 0.045–0.062 Å in **2** than in **1**. This

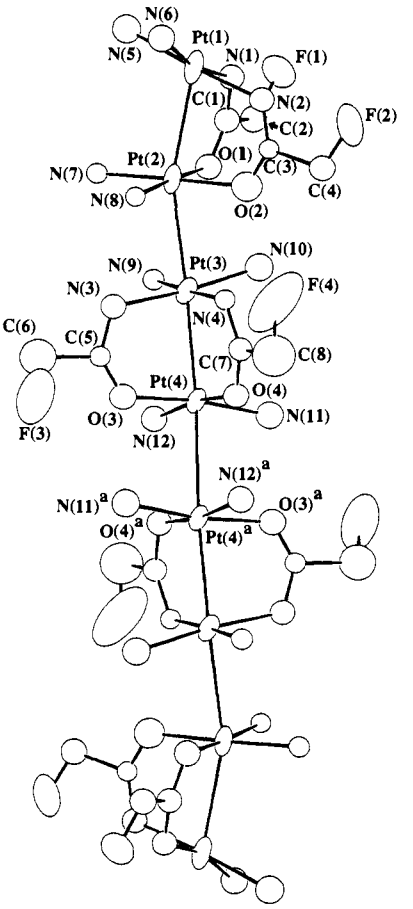

Figure 5. An ORTEP drawing and the atom labeling scheme for the $[(H_3N)_2Pt(CH_2FCONH)_2Pt(NH_3)_2]_4^{8.66+}$ (**2c**).

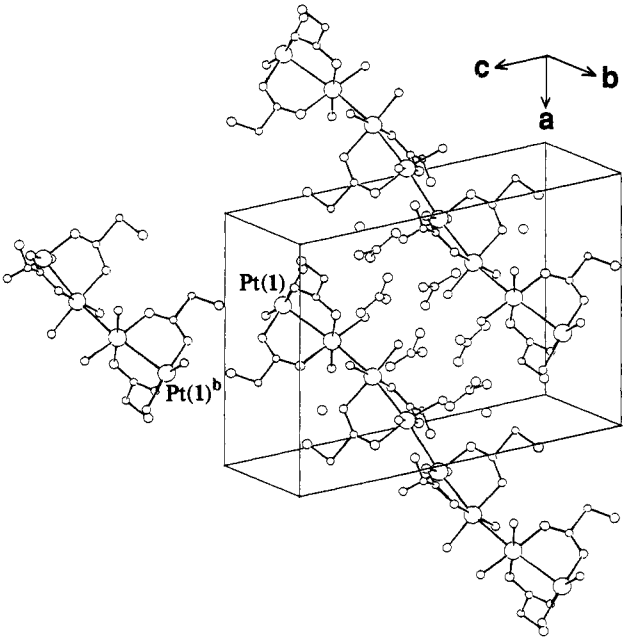

Figure 6. The crystal packing and the intercationic relationship in **2**.

fact is the result of a lower average Pt oxidation state of **2**. A similar relationship between the average Pt oxidation state and the Pt–Pt distance is observed in amidate-bridged tetranuclear platinum blues and related compounds.[6-10] However, this is the first observation of such relationship in octanuclear platinum compounds.

Magnetic Properties. Although some preparative batches of **1** showed very weak ESR signals ($g_\perp$ = 2.44 and $g_\parallel$ = 1.99),

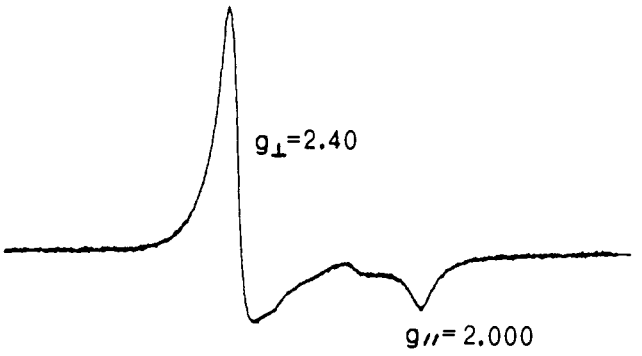

Figure 7. ESR spectrum of **2** in the solid state at 300 K.

typical of those for the tetranuclear platinum blues,[6b,7b,9,32] the integrated intensities were only a few percents per platinum atom, compared to that of *cis*-diammineplatinum α-pyridone blue, $[Pt_4(NH_3)_8(C_5H_4NO)_4]^{5+}$,[7b] and, therefore, the very weak paramagnetism is probably due to a trace of impurity, and compound **1** is considered to be diamagnetic.

Compound **2** is paramagnetic, and the ESR spectrum measured with the microcrystalline sample is shown in Figure 7. The spectrum is consistent with a single unpaired electron per molecule and the unpaired electron resides in d_{z^2} orbitals. However, the integrated intensity of the signal per molecule is ca. 68% of that for the previously reported α-pyridonate-bridged platinum blue, $[Pt_4(NH_3)_8(C_5H_4NO)_4]^{5+}$,[7b] whose spectrum was measured and compared on the same ESR measurement conditions. From these facts it is inferred that the nonoxidized isostructural and diamagnetic Pt(2.0+)$_8$ complex $[(H_3N)_2Pt(CH_2FCONH)_2Pt(NH_3)_2]^{4+}$ is partially mixed in the paramagnetic Pt(2.125+)$_8$ complex $[(H_3N)_2Pt(CH_2FCONH)_2Pt(NH_3)_2]_4^{9+}$ (Pt(2.125+)$_8$ corresponds to one Pt(III) and seven Pt(II) atoms in the octanuclear molecule). Magnetic susceptibility measurement of **2** on a vibrating-sample magnetometer shows that the compound obeys simple Curie paramagnetism down to 4.2 K. The obtained magnetic moment of μ_{eff} = 1.41 μ_B can provide the weight ratio of Pt(2.125+)$_8$ complex in **2**, assuming that the pure paramagnetic Pt(2.125+)$_8$ compound has a magnetic moment of μ_{eff} = 1.73 μ_B. The calculated result was 65.77%, which is in good agreement with the result of the ESR study. Thus, compound **2** can be regarded as a mixture of diamagnetic Pt(2.0+)$_8$ and paramagnetic Pt(2.125+)$_8$ complexes. Compound **2** is the first example of a paramagnetic octanuclear platinum complex and is contrasted to the diamagnetic compound **1**. A similar mixture of the tetranuclear platinum blues with different average Pt oxidation states has been reported previously.[32] The formula and the nonstoichiometric number of the nitrate anions in **2** have been determined based on the magnetic susceptibility measurement. X-ray diffraction analysis of **2** shows the existence of six nitrate groups per octanuclear complex, and the remaining nitrate ions seem to be disordered in the crystal lattice. The samples used for the X-ray analysis and for the magnetic susceptibility measurement were identical, which was confirmed with the elemental analysis, and there was not any difference of the samples between different preparative batches. The lower average Pt oxidation state of **2**, compared to that of **1**, would be a result of the poorer donating ability of the 2-fluoroacetamidate ligand. The electron-withdrawing nature of the F atoms makes **2** more resistant to oxidation, compared to **1**, thus lowering the average Pt oxidation state.

Solid State Electronic Spectra and Extended Hückel Molecular Orbital Description. Figure 8 (parts a and b) shows the single-crystal transmittance and reflectance spectra of **1**, respectively. Figure 8c is the absorption spectrum of **1**, which was calculated and constructed from Figure 8a. The diffuse reflectance spectrum of the microcrystalline sample of **1** in the range of 200–1600 nm is shown in Figure 9. Figures 8 and 9 show that **1** has a strong

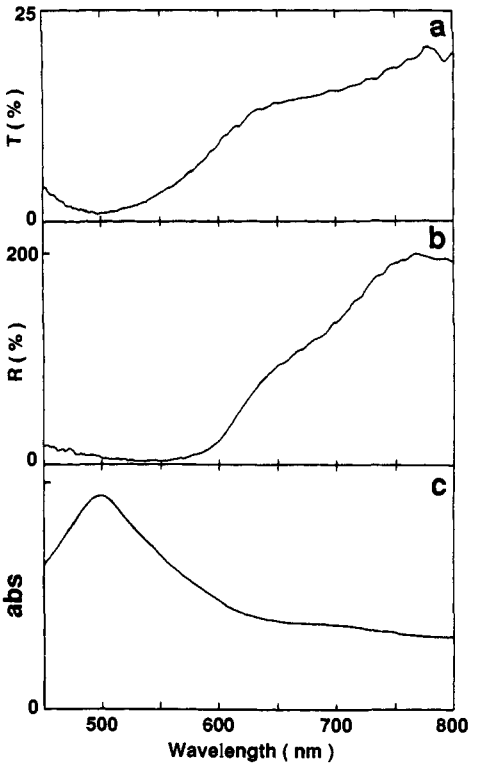

Figure 8. The spectra of a single crystal of **1** measured on a Hitachi U-6000 spectrophotometer: (a) transmittance spectrum, (b) diffuse reflectance spectrum, and (c) absorption spectrum calculated from (a).

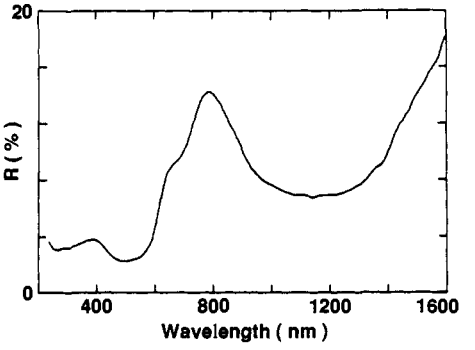

Figure 9. The diffuse reflectance spectrum of **1** measured on a Shimadzu UV3101PC spectrophotometer.

broad absorption band in the range of 450–650 nm with λ_{max} = 500 nm, which approximately corresponds to the value of λ_{max} = 540 nm observed during the synthesis (Figure 1). Figures 8 and 9 also show a relatively weak absorption band in the range of 650–750 nm. These strong absorption bands in the visible region are similarly observed in the tetranuclear platinum blues[6,7b,33] and are attributed in the tetranuclear compounds to the intervalence transitions between the orbitals which are mainly composed of d orbitals of the platinum atoms and are delocalized over the four platinum atoms.[34] In the octanuclear compound **1**, another strong broad band is observed, as shown in Figure 9, at around 1200 nm (λ_{max} = 1140 nm). Such absorption band in the near infrared region has not been observed for the tetranuclear platinum blues and tan and would be the typical feature of the octanuclear Pt chain compounds. The transmittance and reflectance spectra of **2** are shown in Figure 10.

In order to understand the nature of the absorption bands in the near infrared region, EHMO calculation was performed for

(32) Matsumoto, K.; Takahashi, H.; Fuwa, K. *J. Am. Chem. Soc.* **1984**, *106*, 2049.

(33) Matsumoto, K.; Watanabe, T. *J. Am. Chem. Soc.* **1986**, *108*, 1308.
(34) Ginsberg, A. P.; O'Halloran, T. V.; Fanwick, P.; Hollis, L. S.; Lippard, S. J. *J. Am. Chem. Soc.* **1984**, *106*, 5430.

Table III. Orbitals with Significant d_{z^2} Contribution and with Involvement in the Electronic Absorption Bands

orbital	energy, eV	interactions[a] Pt(1)–Pt(2)	Pt(2)–Pt(3)	Pt(3)–Pt(4)	Pt(4)–Pt(4′)
87	−13.98	σ, δ	σ	σ*	σ*
90	−13.97	σ	σ*, π	σ, π, δ	σ, π, δ
137	−13.21	π(s), δ	π(s), δ(s)	π(s), δ(s)	σ(s), π(s), δ(s)
138	−13.04	σ(s), π(s), δ(s)	π(s), δ(s)	π(s), δ(s)	σ*, π*(s), δ*(s)
156 (HOMO)	−12.21	σ*(s), π*(s), δ*(s)	σ(s), π(s), δ(s)	σ*, π*, δ*(s)	σ, π, δ(s)
157 (LUMO)	−12.15		δ*	σ(s), π(s), δ	σ*(s), π*(s), δ*
159	−12.11	σ*, π, δ(s)	π	π*, δ	π, δ(s)
160	−12.11	σ*, π*(s), δ(s)	σ*, π*, δ*(s)	σ*, π, δ*(s)	π*, δ*(s)
161	−12.05	π, δ(s)	π*(s), δ*(s)	σ, π, δ(s)	σ*, π*, δ*(s)
162	−12.04	σ(s), π(s), δ	σ, π	σ, π, δ(s)	σ, π, δ(s)
163	−12.03	σ(s), π	σ*(s), π*	σ, π(s), δ(s)	σ, π(s), δ(s)

[a] Small letter s in the bracket shows that the interaction is strong.

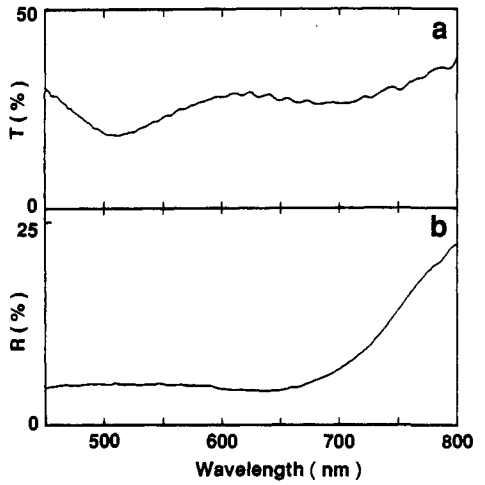

Figure 10. The spectra of a single crystal of **2**: (a) transmittance spectrum and (b) diffuse reflectance spectrum.

1 including all the atoms except the methyl and ammine hydrogen atoms in the complex cation. The result shows a number of energy levels with the energy separations of the order of 0.01 eV between the adjacent levels. Significant contributions of the Pt 5d orbitals approximately start at MO 75 (−14.81 eV) and continue to MO 200 (−8.51 eV). The HOMO 175 (−12.21 eV) is mainly composed of Pt 5d orbitals as shown in Table III. The energy gap between the HOMO and LUMO (−12.15 eV) is only 0.055 eV, showing the very crowded, band-like structure of the MOs. Table IV shows the assignments of the absorption bands, which was determined referring to the calculated transition moments. Table III lists the MOs having significant d_{z^2} contributions and being involved in the electronic absorption bands. It is clear that the absorption band at around 500 nm corresponds to the transitions from MOs composed of Pt d orbitals (87, 90) or Pt d orbitals plus ligand orbitals (75, 76, 79) to MOs composed of Pt d orbitals. All of the MOs involved in the transitions at around 1140 nm, which is the typical feature of the octanuclear chain structure, are significantly of Pt d orbital nature, and the transitions correspond to the charge transfers between the Pt atoms in the octanuclear chain. Especially, the transitions 137 → 161, 137 → 157, 138 → 162, and 138 → 159 in the near infrared region are considerably dominated by the charge transfers along the Pt–Pt bonding axes. The nature of the transitions in the near infrared region described above is basically the same with those observed in the visible region for α-pyridonate-bridged tetranuclear platinum blue, which was explained by EHMO[5d] or SCF-Xα[9,34] calculations. It is no wonder that the lowest transition energy is shifted from visible to near infrared region on going from the tetranuclear to the octanuclear compound, since the transition energies of this sort of compounds can be approximately calculated with a simple one-dimensional model for a particle in a one-dimensional box of length L (L corresponds to the sum of the d_{z^2} orbitals for the entire platinum chain).[9]

Table IV. Electronic Absorption Bands and the Assignments for **1**

obsd values λ_{max}, nm	energy, eV	intensity	transition	calcd values λ_{max}, nm	energy, eV	intensity
~500	~2.48	vs	76 → 162	448	2.76	vs
			75 → 161	449	2.76	vs
			75 → 160	459	2.70	s
			79 → 159	483	2.57	s
			87 → 162	638	1.94	s
			90 → 163	639	1.94	s
			90 → 161	643	1.93	vs
~1140	~1.09	s	126 → 157	932	1.33	s
			131 → 160	1056	1.17	s
			132 → 159	1061	1.17	s
			137 → 161	1066	1.16	s
			135 → 157	1157	1.07	s
			137 → 157	1171	1.06	s
			138 → 162	1238	1.00	s
			138 → 159	1332	0.93	s

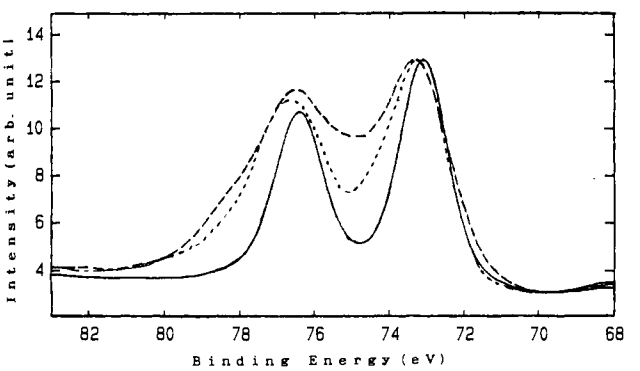

Figure 11. X-ray photoelectron spectra of H–H $[Pt_2(en)_2(\alpha\text{-pyridonato})_2](NO_3)_2$ (—), $[Pt_4(NH_3)_8(\alpha\text{-pyrrolidonato})_4](ClO_4)_2(NO_3)_3 \cdot 5H_2O$ (– –), and **1** (— —).

X-ray Photoelectron Spectra of Amidate-Bridged Binuclear, Tetranuclear, and Octanuclear Platinum Compounds. The X-ray photoelectron spectra of several amidate-bridged binuclear, tetranuclear, and octanuclear platinum compounds were measured in order to know the degree of the mixed-valency of the compounds and the effect of the nuclear number of the compounds on the spectra. Table V summarizes the binding energies of Pt $4f_{5/2}$ and Pt $4f_{7/2}$ photoelectrons. Those of C 1s, N 1s, and O 1s photoelectrons are normal[35] and are not included in the table. Figure

(35) (a) Wagner, C. D.; Riggs, W. M.; Davis, L. E.; Moulder, J. F.; Muilenberg, G. E. *Handbook of X-ray Photoelectron Spectroscopy*; Perkin-Elmer Co., Physical Electronics Division: USA, 1979. (b) Clark, D. T.; Adams, I.; Briggs, D. *J. Chem. Soc., Chem. Commun.* **1971**, 603. (c) Cahen, D.; Lester, J. E. *Chem. Phys. Lett.* **1973**, *18*, 109. (d) Escard, J.; Pontvianne, B.; Contour, J. P. *J. Electron. Spectrosc.* **1975**, *6*, 17. (e) Hommond, J. S.; Winograd, N. *J. Electroanal. Chem. Interfacial Electrochem.* **1977**, *80*, 123. (f) Kim, K. S.; Winograd, N.; Davis, R. E. *J. Am. Chem. Soc.* **1971**, *93*, 6296. (g) Leigh, G. J.; Bremser, W. *J. Chem. Soc., Dalton Trans.* **1972**, 1217.

Table V. Electron Binding Energies of Platinum Blues and Related Compounds

compounds	av Pt ox state	Pt 4f 5/2 (eV)	Pt 4f 7/2 (eV)
H-H[$Pt_2(en)_2(\alpha$-pyridonato)$_2$]$(NO_3)_2$	2.0	76.4	73.1
H-H[$(NO_3)Pt_2(NH_3)_4(\alpha$-pyrrolidonato)$_2(NO_2)$]$(NO_3)_2\cdot H_2O$	3.0	77.9	74.6
[$Pt_4(NH_3)_8(\alpha$-pyrrolidonato)$_4$]$(PF_6)_2(NO_3)_{2.56}\cdot 5H_2O$	2.14	76.4	73.2
[$Pt_4(NH_3)_8(\alpha$-pyrrolidonato)$_4$]$(ClO_4)_2(NO_3)_3\cdot 5H_2O$	2.25	76.7	73.3
[$Pt_4(NH_3)_8(\alpha$-pyrrolidonato)$_4$]$(NO_3)_6\cdot 2H_2O$	2.5	76.7	73.5
1	2.25	76.5	73.3
2	2.08	76.4	73.4

11 shows the spectra of the Pt(II) dimer compound H-H [$Pt_2(en)_2(\alpha$-pyridonato)$_2$]$(NO_3)_2$, the tetranuclear Pt(2.25+) compound [$Pt_4(NH_3)_8(\alpha$-pyrrolidonato)$_4$]$(ClO_4)_2(NO_3)_3\cdot 5H_2O$, and **1**.

The Pt 4f binding energies of the Pt(II) dimer compound are typical of the Pt(II) complexes; for example, those of *cis*-Pt-$(NH_3)_2Cl_2$ are 76.1 and 72.8 eV for $4f_{5/2}$ and $4f_{7/2}$, respectively.[6a] The pure Pt(III) dimer compound, H-H [$(NO_3)Pt_2(NH_3)_4(\alpha$-pyrrolidonato)$_2(NO_2)$]$(NO_3)_2\cdot H_2O$, shows the Pt $4f_{5/2}$ and $4f_{7/2}$ binding energies of 77.9 and 74.6 eV, respectively, which are definitely different from those of the Pt(II) compound or Pt(IV) compounds. The latter compounds usually have their Pt $4f_{5/2,7/2}$ binding energies at 78.7 and 75.4 eV, respectively, which are higher by about 2.5 eV than those of *cis*-$PtCl_2(NH_3)_2$. The $4f_{5/2,7/2}$ binding energies of the Pt(III) dimer compound measured in the present study are more close to those of another Pt(III) dimer compound, $K_2Pt_2(SO_4)_4\cdot 3H_2O$, whose Pt $4f_{5/2}$ and $4f_{7/2}$ binding energies are 78.5 and 75.2 eV.[6a]

The Pt $4f_{7/2}$ binding energy is more sensitive than the Pt $4f_{5/2}$ binding energy to the Pt oxidation state and is usually used to prove the real electronic state of the platinum atom. Looking at the Pt $4f_{7/2}$ binding energies of the three mixed-valent tetranuclear compounds in Table V, one notices that the energies are similar to those of Pt(II) compounds rather than those of Pt(III) ones, and the Pt $4f_{7/2}$ binding energies of the two octanuclear compounds are also close to those of Pt(II) compounds. The values of **1** and **2** lie rather in the opposite order if one considers their average Pt oxidation states, but this might be caused by the higher degree of the spectral overlaps of the Pt(II) peaks and probably of the Pt(III) peaks in the octanuclear compounds, as observed in Figure 11.

Finally, we would like to mention about the spectral shapes of these mixed-valent tetranuclear and octanuclear compounds. As Figure 11 shows, with the increase of the nuclear number from the tetranuclear to the octanuclear compounds, the dented portion between the Pt $4f_{5/2}$ and $4f_{7/2}$ peaks becomes higher, even if the average Pt oxidation state is retained. We consider that the lesser dented part would be reflecting that the contribution of the Pt(III) $4f_{7/2}$ peaks is significantly high and these peaks overlap on the Pt(II) 4f peaks. The octanuclear compounds have four different Pt atoms with different chemical environments, whereas the tetranuclear compounds have two chemically different Pt atoms and these facts would be the cause of the more broadened and lesser dented peak profiles of the octanuclear compounds. Similar spectral overlap of the Pt 4f component in the compounds whose Pt oxidation state is higher than Pt(II) were reported previously;[6a,36] however, the present study more specifically shows that the higher component would be Pt(III) state, by measuring the amidate-bridged Pt(III) dimer compound with ligands of the similar kinds. However, it is not clear at the moment how the average Pt oxidation state, the mixed valency of the compound, and the X-ray photoelectron spectrum correlates with each other. In order to gain the information about the real electronic states of these compounds, we are currently carrying out the spectral analysis including the deconvolution and simulation of the spectra for a wider variety of platinum blues and the related compounds, and the result will be published separately.

Acknowledgment. We thank Prof. K. Kon of the Department of Physics, Waseda University, for his kind help in measuring the magnetic moment of the compound. This work is financially supported by Grant-in-Aids for Scientific Research on Priority Area of "Multiplex Organic Systems" (01649008) and "Bioinorganic Chemistry" (03241101) from the Ministry of Education, Science, and Culture, Japan.

Supplementary Material Available: Details of the crystal data collection procedures for **1** and **2** in Table S1, final atomic positional and thermal parameters for **1** and **2** in Tables S2 and S3, respectively, interatomic distances and angles for **1** and **2** in Tables S4 and S5, respectively, the anisotropic thermal parameters for **1** and **2** in Tables S6 and S7, and the torsion angles about the Pt–Pt axes for **1** and **2** in Tables S10 and S11 (25 pages); structure factor tables for **1** and **2** in Tables S8 and S9 (39 pages). Ordering information is given on any current masthead page.

(36) Burness, J. H. *Inorg. Chim. Acta* **1980**, *44*, L49.